Optical Investigation of $Na_2V_3O_7$ Nanotubes

J. Choi and J. L. Musfeldt

Department of Chemistry, The University of Tennessee, Knoxville, Tennessee 37996

Y. J. Wang

National High Magnetic Field Laboratory, Florida State University, Tallahassee, Florida 32306

H.-J. Koo and M.-H. Whangbo

Department of Chemistry, North Carolina State University, Raleigh, North Carolina 27695

J. Galy and P. Millet

Centre d'Elaboration de Matériaux et d'Eudes Structurales CNRS, 29 rue Jeanne Marvig, BP 4347, 31055 Toulouse Cedex 4, France

Received October 1, 2001. Revised Manuscript Received November 13, 2001

We report the electronic and vibrational properties of $Na_2V_3O_7$ nanotubes and compare the response with other layered and nonlayered vanadates. The electronic structure of $Na_2V_3O_7$ displays a strong similarity to that of nontubular vanadates. We assign the 1.2-eV band as a V d → d excitation and the 3.3- and 3.9-eV bands as O 2p → V 3d charge-transfer structures. Although band structure calculations predict additional fine structure in the density of states because of the tubular morphology, such features are not observed in the absorption spectrum. The vibrational spectrum displays triplet mode splitting as a result of reduced site symmetry, consistent with the three sightly different vanadium atoms that form the basic structural unit. A low-frequency rattling mode is observed in $Na_2V_3O_7$ at 88 cm^{-1}. This unique characteristic of the Na^+-ion intercalated tubes might be connected with the ionic conductivity.

I. Introduction

The discovery of carbon nanotubes opened a completely new chapter in the field of novel carbon materials.[1−4] In analogy with carbon nanotubes, it has been anticipated that other two-dimensional layered compounds can be "rolled up" to form fullerene-like structures, including tubes, scrolls, and onions.[5,6] The rich chemistry of transition metal oxides makes this scenario very attractive. Inorganic materials also undergo facile exchange reactions, e.g., intercalation of various cations during synthesis processes, imparting additional tunable functionality.[7] Further, morphological control of the nanostructure and control of the carrier/spin density (via doping) are expected to provide insight into such properties as superconductivity, density waves, and quantum magnetism. At the same time, exciting new opportunities to exploit these physical characteristics might emerge.

The first inorganic (WS_2) nanotubes were synthesized in 1992.[5] Since this time, a handful of other mesoscopic metal dichalcogenides have been investigated as allotropes of two-dimensional layered materials.[8] These include MoS_2, where, despite the tube curvature, the interatomic distance are quite similar to those in the two-dimensional analog.[5,9−11] Other similar compounds, including WS_2, Si- and P-based tubes, GaSe, and NbS_2, as well as MoS_2, have received theoretical attention.[12−15] Here, calculations predict both direct and indirect band

(1) Iijima, S. *Nature* **1991**, *354*, 56.
(2) Mintmire, J. W.; Dunlap, B. I.; White, C. T. *Phys. Rev. Lett.* **1992**, *68*, 631.
(3) Guo, T.; Nikolaev, P.; Thess, A.; Colbert, D. T.; Smalley, R. E. *Chem. Phys. Lett.* **1995**, *243*, 49.
(4) Dresselhaus, M. S.; Dresselhaus, G.; Eklund, P. C. *Science of Fullerenes and Carbon Nanotubes*; Academic Press: New York, 1996.
(5) Tenne, R.; Margulis, L.; Genut, M.; Hodes, G. *Nature* **1992**, *360*, 444.
(6) Margulis, L.; Salitra, G.; Tenne, R.; Talianker, M. *Nature* **1993**, *365*, 114.
(7) Muhr, H.-J.; Krumeich, F.; Schonhölzer, U. P.; Bieri, F.; Niederberger, M.; Gauckler, L. J.; Nesper, R. *Adv. Mater.* **2000**, *12*, 231.
(8) In carbon-based nanotubes, it is well-known that the size of the gap depends critically on the tube diameter and the chirality. Thus far, the inorganic tubes seem more consistent in terms of "quality control" during production; single-phase material is generally obtained, giving the advantage of uniform (rather than mixed) tube characteristics.
(9) Frey, G. L.; Elani, S.; Homyonfer, M.; Feldman, Y.; Tenne, R. *Phys. Rev. B* **1998**, *57*, 6666.
(10) Seifert, G.; Terrones, H.; Terrones, M.; Jungnickel, G.; Frauenheim, T. *Phys. Rev. Lett.* **2000**, *85*, 146.
(11) Seifert, G.; Frauenheim, T.; Köhler, T.; Urbassek, H. M. *Phys. Status Solidi B* **2001**, *225*, 393. Remskar, M.; Mrzel, A.; Skraba, Z.; Jesih, A.; Ceh, M.; Demšàr, J.; Stadelmann, P.; Lévy, F.; Mihailovic, D. *Science* **2001**, *292*, 479.
(12) Côté, M.; Cohen, M. L.; Chadi, D. J. *Phys. Rev. B* **1998**, *58*, 4277.
(13) Seifert, G.; Köhler, T.; Urbassek, H. M.; Hernández, E.; Frauenheim, T. *Phys. Rev. B* **2001**, *63*, 193409.
(14) Seifert, G.; Hernández, E. *Chem. Phys. Lett.* 2000, *318*, 355.
(15) Seifert, G.; Terrones, H.; Terrones, M.; Frauenheim, T. *Solid State Commun.* **2000**, *115*, 635. Seifert, G.; Terrones, H.; Terrones, M.; Jungnickel, G.; Fraunheim, T. *Solid State Commun.* **2000**, *114*, 245.

10.1021/cm010965x CCC: $22.00
Published on Web 01/18/2002

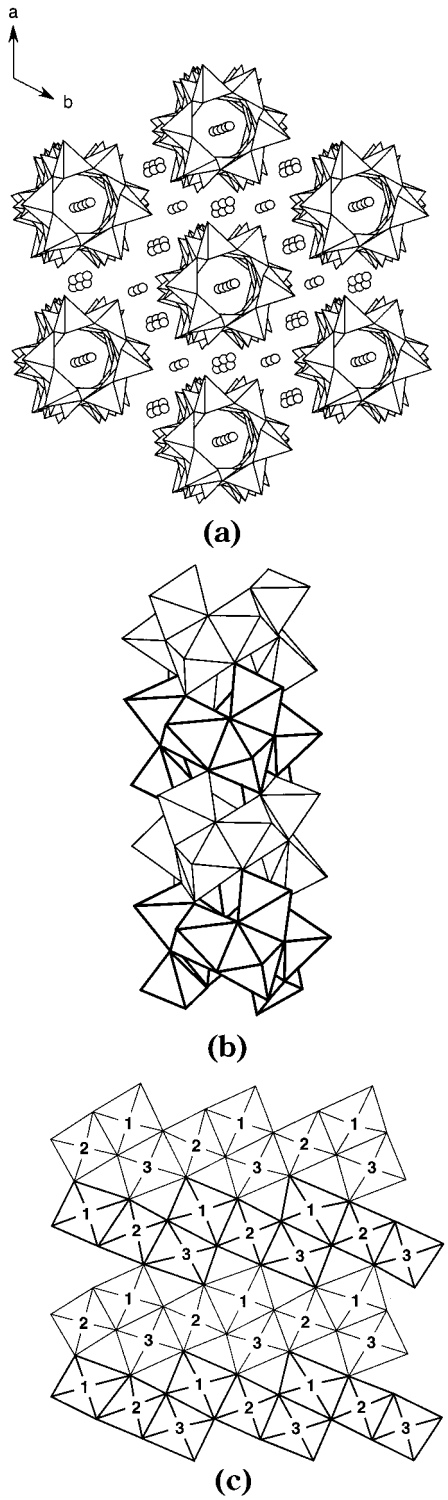

Figure 1. (a) Schematic projection view of the crystal structure of $Na_2V_3O_7$ along the *c* axis, where each nanotube is made up of VO_5 square pyramids represented by polyhedra and each small circle represents an Na atom. (b) Perspective view of a nanotube, where adjacent rings of VO_5 square pyramids are distinguished by polyhedra of thick and thin lines. (c) Planar view of four adjacent rings of the nanotube, where the numbers 1, 2, and 3 indicate that the square pyramids contain V(1), V(2), and V(3) atoms, respectively.

gaps, depending on the material, with the gap energy increasing with the tube diameter toward the bulk limit in certain cases and remaining independent of the tube diameter in other examples.[10,11,16] Other mesoscopic compounds of recent interest include multiwalled $NiCl_2$ nanotubes,[17] inorganic wires and fibers,[18−22] and vanadium oxide (VO_x) scrolls nanotubes.[17] The (VO_x) scrolls have been investigated for their novel electrochemical properties.[23−25] In addition to the aforementioned materials, $Na_2V_3O_7$ nanotubes have recently been synthesized by solid-state reaction.[26] As described in the next paragraphs, these tubes are much more complex than the aforementioned metal dichalcogenides from both chemical and structural points of view.

Vanadates are well-known to display unusual structural and magnetic properties. This is because vanadium ions can exhibit a variety of bonding patterns (resulting in octahedral, tetrahedral, trigonal, and square pyramidal coordination) and often show different or even mixed oxidation states.[27,28] For instance, V_2O_5 is the "parent compound" of a whole family of vanadates; it has a layered structure formed by VO_5 square pyramids. $Na_2V_3O_7$, the material of interest in this work, belongs to this family as well and is attractive as a mesoscopic analogue of V_2O_5. The structure of the title compound is shown in Figure 1. X-ray diffraction reveals that the $Na_2V_3O_7$ tubes are built of both corner- and edge-sharing VO_5 square pyramids. Each vanadium displays a 4+ charge; note that V^{4+} has one 3d-electron with a single unpaired spin. Three unique vanadium atoms [V(1), V(2), and V(3)] form a basic structural unit, and nine square pyramids build a "ring" of the nanotube; two adjacent rings form the unit cell. The inner tube diameter is ∼5 Å,[26] more than 2 orders of magnitude smaller than that of most metal dichalcogenide nanotubes and vanadium oxide scrolls.[23−25] The unfolded geometry of the $Na_2V_3O_7$ sheet is very close to that of MV_3O_7 [M = CH_3NH_3 or $N(CH_3)_4$],[28,29] except that pyramidal units in $Na_2V_3O_7$ point in the same direction, whereas those in MV_3O_7 point in opposite directions (two apexes up and two apexes down).

In addition to the unusual structural properties, many vanadates display exotic magnetic properties.[30−32] Certainly, $Na_2V_3O_7$ is no exception. Early dc-susceptibility studies indicated antiferromagnetic behavior at high temperatures, with a change in magnetic properties

(16) Strain energy also decreases as the tube diameter increases.
(17) Rosenfeld Hacohen, Y.; Grunbaum, E.; Tenne, R.; Sloan, J.; Hutchison, J. L. *Nature* **1998**, *395*, 336.
(18) Skomski, R.; Zeng, H.; Zheng, M.; Sellmyer, D. *J. Phys. Rev. B* **2000**, *62*, 3900.
(19) Loiseau, A.; Willaime, F.; Demoncy, N.; Hug, G.; Pascard, H. *Phys. Rev. Lett.* **1996**, *76*, 4737.
(20) Shi, W. S.; Zheng, Y. F.; Wang, N.; Lee, C. S.; Lee, S. T. *J. Vac. Sci. Technol. B* **2001**, *19*, 1115.
(21) Liang, C. H.; Meng, G. W.; Wang, G. Z.; Zhang, L. D.; Zhang, S. Y. *Chem. Mater.* **2001**, *13*, 2150.
(22) Huang, M. H.; Mao, S.; Feick, H.; Yan, H.; Wu, Y.; Kind, H.; Weber, E.; Russo, R.; Yang, P. *Science* **2001**, *292*, 1897.
(23) Spahr, M. E.; Bitterli, P.; Nesper, R.; Müller, M.; Krumeich, F.; Nissen, H. U. *Angew. Chem., Int. Ed.* **1998**, *37*, 1263.
(24) Nesper, R.; Muhr, H.-J. *Chimia* **1998**, *52*, 571.
(25) Krumeich, F.; Muhr, M.-J.; Niederberger, M.; Bieri, F.; Schnyder, B.; Nesper, R. *J. Am. Chem. Soc.* **1999**, *121*, 8324.
(26) Millet, P.; Henry, J. Y.; Mila, F.; Galy, J. *J. Solid State Chem.* **1999**, *147*, 676.
(27) Zavalij, P. Y.; Zhang, F.; Whittingham, M. S. *Acta Crystallogr.* **1999**, *B55*, 953; *J. Solid State Chem.* **1999**, *147*, 676.
(28) Chirayil, T.; Zavalij, P.; Whittingham, M. S. *Chem. Mater.* **1998**, *10*, 2629.
(29) Chen, R.; Zavalij, P. Y.; Whittingham, M. S.; Greedan, J. E.; Raju, N. P.; Bieringer, M. *J. Mater. Chem.* **1999**, *9*, 93.
(30) Ueda, Y. *Chem. Mater.* **1998**, *10*, 2653.
(31) Lumsden, M. D.; Sales, B. C.; Mandrus, D.; Nagler, S. E.; Thompson, J. R. *Phys. Rev. Lett.* **2001**, *86*, 159.
(32) Choi, J.; Musfeldt, J. M.; Ragghianti, G.; Mandrus, D.; Sales, B. C.; Thompson, J. R. *Phys. Rev. B*, manuscript accepted.

below 100 K.[33] Preliminary spin−lattice relaxation measurements did not identify a spin gap.[33] On the basis of its similarity with other layered vanadates, Millet et al. proposed that the magnetic structure of $Na_2V_3O_7$ could be considered within an $S = {}^1/_2$ three-legged ladder model, with periodic boundary conditions in the rung direction.[26] More recently, Whangbo et al. suggested a model of the spin-exchange interactions described by six mutually intersecting helical chains that can be approximated as a single helical chain at low temperature.[34] In this model, each helical chain is described by four antiferromagnetic spin-exchange parameters; antiferromagnetically ordered spins form the spin singlet ground state, and flipping one of the four spins gives rise to an excited state. Both models predict the existence of a spin gap, although neither framework estimates the gap size.[26,34] Judging from the typical energy scale of magnetic interactions, it is likely that such a spin gap would be found in the millimeter or far-infrared frequency range.

Despite the fascinating morphology, the striking magnetic properties predictions, and the overall similarity with other vanadates, the physical properties of mesoscopic $Na_2V_3O_7$ are almost wholly unknown. Further, few detailed spectroscopic investigations of the important and rapidly growing class of complex inorganic nanomaterials have been carried out.[9] Such measurements are important for understanding more refined calculations on complex tubes. In this work, we investigate the electronic and vibrational properties of $Na_2V_3O_7$, and we compare the results with those of similar layered and nonlayered (but nontubular) vanadates. In search of the predicted spin gap, we also measure the magnetic field dependence of the far-infrared transmittance.

II. Experimental Section

Single crystals of $Na_2V_3O_7$ were grown under vacuum in a tubular furnace from a melt with the starting composition $Na_{1.9}V_2O_5$. The resultant material was harvested as black fibrous bundles, with typical dimensions of $2 \times 2 \times 5$ mm^3. The bundles break easily into individual crystal fibers with diameters of less than 100 μm.

Although polarized reflectance measurements were desirable because of the high anisotropy of the fibrous bundles, we were unable to obtain reliable data on account of overall low reflection and strong scattering from the rough surface. Thus, we elected to pursue transmittance experiments. For these measurements, $Na_2V_3O_7$ was ground with both paraffin and dry KCl powder and then pressed under vacuum at 7000 and 20 000 psi to form isotropic pellets for far- and middle-infrared measurements, respectively. The $Na_2V_3O_7$ concentrations were 13 wt % in paraffin and 500 ppm in KCl. The absorption coefficient was calculated from transmittance as

$$\alpha(\omega) = -\frac{1}{hd} \ln T(\omega)$$

where h is the concentration of $Na_2V_3O_7$ in the matrix, and d is the pellet thickness.[35]

Infrared measurements were carried out using a Bruker 113 V Fourier transform infrared spectrometer equipped with 23-μm Mylar, 6-μm broad band, and KBr beam splitters, covering the frequency range from 30 to 5000 cm^{-1}. Both bolometer (far-infrared) and DTGS (middle-infrared) detectors were employed. A modified Perkin-Elmer Lambda 900 grating spectrometer was used to cover the high-energy range (0.5−5 eV). Resolution was 1−2 cm^{-1} (as needed in the far- and middle-infrared) and 2 nm (near-infrared to near-ultraviolet). Low-temperature measurements were carried out with a continuous-flow helium cryostat. The advantage of low-temperature spectroscopy is that diffuse electronic structure tends to sharpen and detailed fine structure in the vibrational response can be resolved.

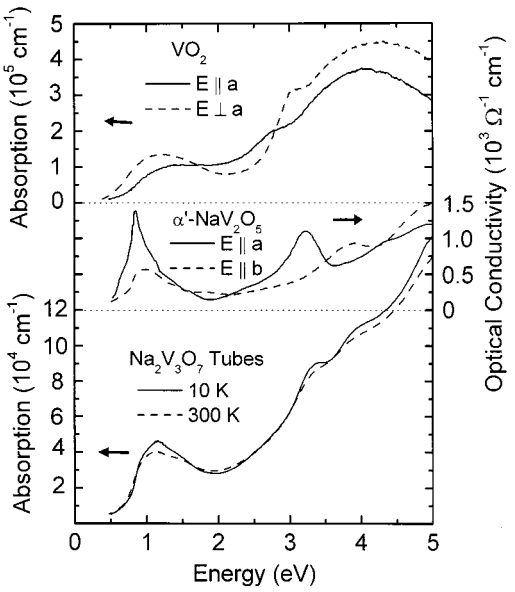

Figure 2. Optical absorption spectra of $Na_2V_3O_7$ in a KCl pellet at 10 K (solid line) and 300 K (dashed line). For comparison, the polarized optical conductivity of α'-NaV_2O_5 in the $E||a$ (solid line) and $E||b$ (dashed line) polarizations[40] and the 300-K absorption spectra of VO_2 in the $E||a$ (solid line) and $E\perp a$ (dashed line) polarizations[41] are also presented.

The magnetooptics experiments were performed at the National High Magnetic Field Laboratory in Tallahassee, Florida, using a 20-T superconducting magnet and a Bruker 113 V instrument. The setup is described in detail elsewhere.[36] All data were collected in transmittance mode at 4.2 K. To detect any small, field-dependent features, transmittance ratios $T(H, 4.2\text{ K})/T(H{=}0, 4.2\text{ K})$ were calculated. Deviations of this normalized response from unity with applied fields might be taken to suggest the presence of a spin gap.

Electronic structure calculations were carried out using the extended Hückel tight-binding method. This method has been shown to be successful in the past for understanding the behavior of other transition metal oxides.[37−40]

III. Results and Discussion

A. Electronic Structure of $Na_2V_3O_7$ Nanotubes. Figure 2 displays the optical absorption spectrum of $Na_2V_3O_7$ at 300 and 10 K. Three fairly prominent and broad bands are observed at ∼1.2, 3.3, and 3.9 eV. These

(33) Gavilano, J. L.; Rau, D.; Mushkolaj, S.; Ott, H. R.; Millet, P.; Mila, F. *Physica B*, manuscript submitted.

(34) Whangbo, M.-H.; Koo, H.-J. *Solid State Commun.* **2000**, *115*, 675.

(35) Wooten, F. *Optical Properties of Solids*; Academic Press: New York, 1972.

(36) Ng, H. K.; Wang, Y. J. *Physical Phenomena at High Magnetic Fields II*; Fisk, Z., Gor′kov, L., Meltzer, D., Schrieffer, R., Eds.; World Scientific: Singapore, 1995; p 729.

(37) Whangbo, M.-H. *Theor. Chem. Acc.* **2000**, *103*, 252.

(38) Rudko, G. Y.; Long, V. C.; Musfeldt, J. L.; Koo, H. J.; Whangbo, M. H.; Revcolevschi, A.; Dhalenne, G.; Bernholdt, D. E. *Chem. Mater.* **2001**, *13*, 939.

(39) Jung, D.; Koo, H. J.; Dai, D.; Whangbo, M. H. *Surf. Sci.* **2001**, *473*, 193.

(40) Long, V. C.; Zhu, Z.; Musfeldt, J. L.; Wei, X.; Koo, H.-J.; Whangbo, M.-H.; Jegoudez, J.; Revcolevschi, A. *Phys. Rev. B* **1999**, *60*, 15721.

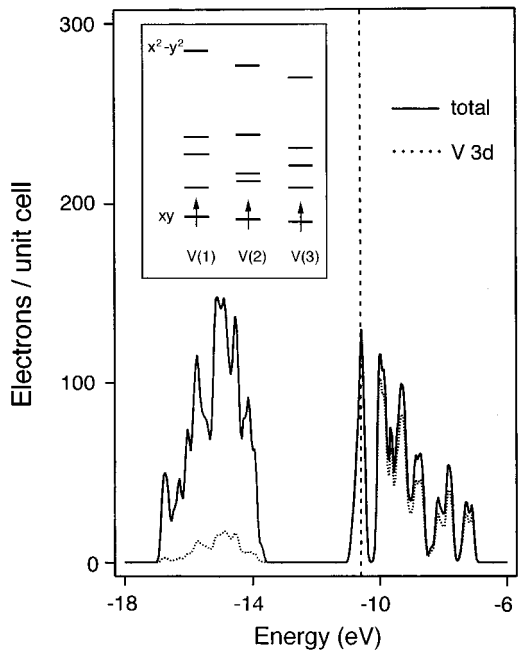

Figure 3. Total density of states (solid line) calculated for the V/O lattice of $Na_2V_3O_7$, where the V 3d orbital contribution is given by the dotted line. The inset shows the relative orderings of the d-block levels calculated for the V(i)O_5 (i = 1−3) square pyramids. For the V(2)O_5 square pyramid, the second, third, and fourth levels exhibit the *xz*, *yz*, and z^2 orbital characters, respectively. These three orbital characters appear mixed in the corresponding levels of the V(2)O_5 and V(2)O_5 pyramids because of their stronger distortions.

structures sharpen only modestly at low temperatures. For comparison, the electronic structures of VO_2[41] and α′-NaV_2O_5 in the $E||a$ and $E||b$ polarizations[40,43] are also included in the plot.

Figure 3 displays the electronic structure calculated for the V/O lattice of $Na_2V_3O_7$ using the extended Hückel tight-binding method. Both p and d blocks are shown. The p block is observed below −14 eV, whereas the d block is observed above −11 eV. The relative orderings of the d-block energy levels of the V(i)O_5 (i = 1−3) square pyramids are summarized in the inset of Figure 3. In contrast to results on other layered and nonlayered vanadates, the projected density of states displays a great deal of interesting fine structure, presumably because of the tubular morphology of the material. Such features are, however, not observed in the absorption spectrum (Figure 2).

Despite the obvious structural and charge differences,[44] the overall absorption spectrum of the $Na_2V_3O_7$ nanotubes shows a striking resemblance to that of the other vanadates.[40−42,47] As seen in Figure 2, all three materials display a strong, broad excitation near 1 eV. In VO_2, where all transition metal atoms have a 4+ charge, this feature has been assigned as a localized d → d transition between ground and excited states split by a crystal field.[42] Comparative vacuum-ultraviolet photoemission studies in this vanadate family (VO_2, V_2O_3, V_2O_5, and V_6O_{13}) further illustrate the similarity; the aforementioned 1-eV band is followed by a broader, more intense structure.[42] The response of V_2O_5 is an exception to this trend. Here, the 1-eV band is absent as a result of the material's V^{5+} oxidation state; without d electrons, the V d → d transition is silent. Assignment of the 1-eV excitation in α′-NaV_2O_5 has been controversial.[40,48−52] Nevertheless, the 1-eV excitations of α′-$NaV_2O_5$and $Na_2V_3O_7$ are remarkably similar, suggesting that they might have a similar origin. From a structural point of view, $Na_2V_3O_7$ is quite different from VO_2, V_2O_5, and α′-NaV_2O_5; however, the electron configuration of the title compound is most similar to that of VO_2. Figure 3 shows that, in each V(i)O_5 square pyramid of $Na_2V_3O_7$, the d_{xy} bands are well separated from the remaining d-orbital bands. There are strong density-of-state (DOS) peaks approximately 1−1.5 eV above the d_{xy} bands. Therefore, we assign the 1.2-eV band in $Na_2V_3O_7$ as a localized d → d transition between crystal field split levels.

The higher-energy features of $Na_2V_3O_7$ are also strikingly similar to those of α′-NaV_2O_5, the bands near 3.3 and 3.9 eV nearly coinciding with the 3.2- ($E||a$) and 3.9-eV ($E||b$) bands of α′-NaV_2O_5 (Figure 2). Figure 3 suggests that these excitations can be identified as either localized V d → d or O 2p → V 3d charge-transfer transitions. Indeed, such excitations in α′-NaV_2O_5 have been variously interpreted as localized V d → d or O 2p → V 3d charge-transfer transitions.[40,47,48] However, the appearance of the higher-energy band in V_2O_5 seems to exclude the possibility that these structures should be attributed to V d → d transitions in $Na_2V_3O_7$. Therefore, we assign the 3.3- and 3.9-eV bands in $Na_2V_3O_7$ as O 2p → V 3d charge-transfer excitations. These values are in good agreement with the calculated band structure (Figure 3).

Few other optical investigations of inorganic fullerene-like materials have been performed. The most well-studied compounds are MoS_2 and WS_2, which display red-shifted exciton bands with increasing wall thickness. However, $Na_2V_3O_7$ is essentially a single-walled (rather than multiwalled) tube, so a direct comparison of these trends is not possible.

B. Vibrational Response of $Na_2V_3O_7$ Nanotubes. Figure 4 shows the 10-K vibrational response of $Na_2V_3O_7$.

(41) Verleur, H. W.; Barker, A. S., Jr.; Berglund, C. N. *Phys. Rev.* **1968**, *172*, 788.

(42) Shin, S.; Suga, S.; Taniguchi, M.; Fujisawa, M.; Kanzaki, H.; Fujimori, A.; Daimon, H.; Ueda, Y.; Kosuge, K.; Kachi, S. *Phys. Rev. B* **1990**, *41*, 4993.

(43) Here, the optical conductivities of α′-NaV_2O_5 were obtained via Kramers−Kronig analysis of the reflectance spectra.

(44) VO_2 has a metal−insulator transition near 340 K. In the insulating phase below 340 K, its crystal structure is nonlayered and monoclinic. VO_2 has V^{4+}, the same as $Na_2V_3O_7$. The 300-K structure of α′-NaV_2O_5 is orthorhombic with $V^{4.5+}$. Its low-dimensional structure is built of the layers of VO_5 square pyramids stacked along *c* axis, separated by Na atoms. α′-NaV_2O_5 has a transition at 34 K, below which charge ordering appears.[45,46,49]

(45) von Schnering, H. G.; Grin, Y.; Kaupp, M.; Somer, M.; Kremer, R. K.; Jepsen, O.; Chatterji, T.; Weiden, M. *Z. Kristallogr.* **1998**, *213*, 246.

(46) Meetsma, A.; de Boer, J. L.; Damascelli, C.; Jegoudez, J.; Revcolevschi, A.; Palstra, T. T. M. *Acta Crystallogr.* **1998**, *54*, 1558.

(47) Atzkern, S.; Knupfer, M.; Golden, M. S.; Fink, J.; Yaresko, A. N.; Antonov, V. N.; Hübsch, A.; Waidacher, C.; Becker, K. W.; von der Linden, W.; Obermeier, G.; Horn, S. *Phys. Rev. B* **2001**, *63*, 165113.

(48) Presura, C.; van der Marel, D.; Dischner, M.; Geibel, C.; Kremer, R. K. *Phys. Rev. B* **2000**, *62*, 16522.

(49) Smolinski, H.; Gros, C.; Weber, W.; Peuchert, U.; Roth, G.; Weiden, M.; Geibel, C. *Phys. Rev. lett.* **1998**, *80*, 5164.

(50) Damascelli, A.; van der Marel, D.; Gruninger, M.; Presura, C.; Palstra, T. T. M.; Jegoudez, J.; Revcolevschi, A. *Phys. Rev. Lett.* **1998**, *81*, 918.

(51) Horsch, P.; Mack, F. *Eur. Phys. J. B* **1998**, *5*, 367.

(52) Golubchik, S.; Isobe, M.; Ivlev, A. N.; Mavrin, B. N.; Popova, M. N.; Sushkov, A. B.; Ueda, Y.; Vasil'ev, A. N. *J. Phys. Soc. Jpn.* **1997**, *66*, 4042.

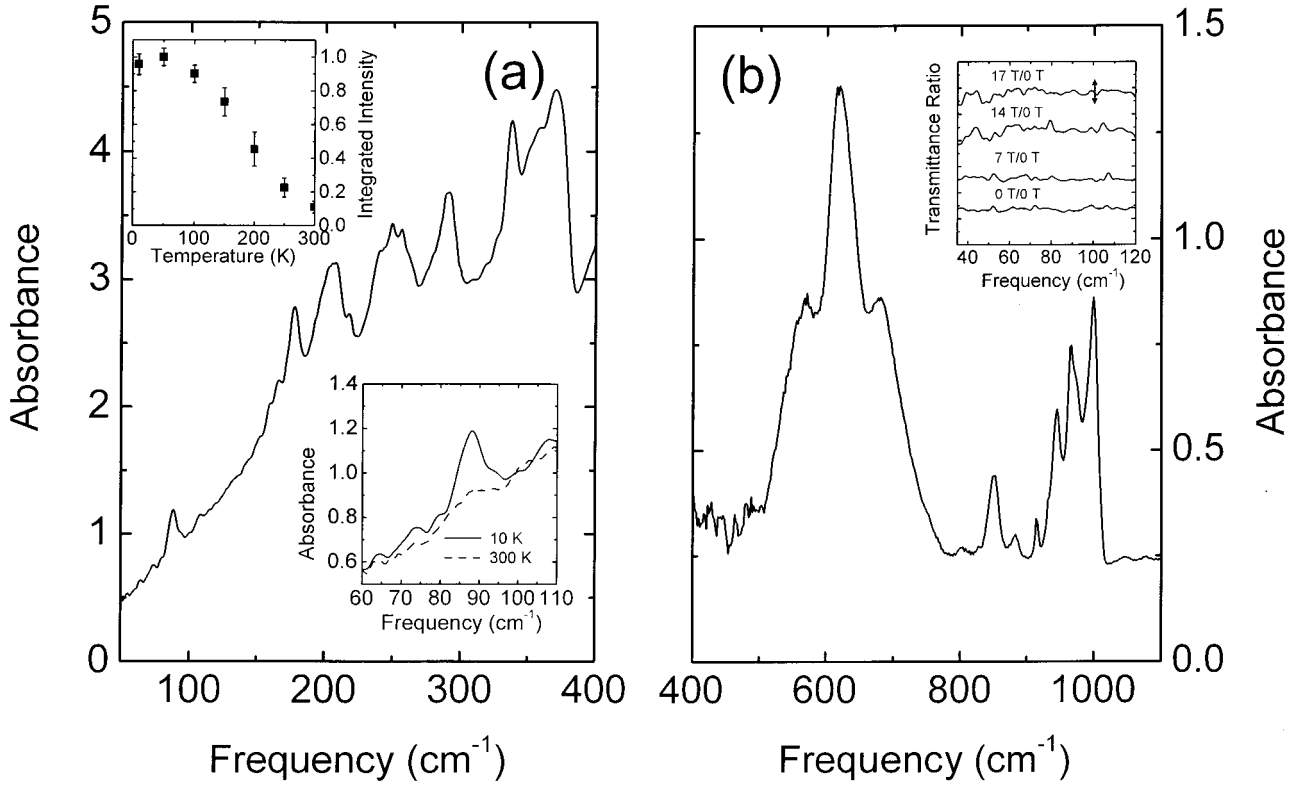

Figure 4. (a) 10-K far-infrared absorption spectrum of $Na_2V_3O_7$ nanotubes in a paraffin matrix. The upper inset shows the integrated intensity of the 88-cm^{-1} mode as a function of temperature. The lower inset displays a close-up view of the 88-cm^{-1} mode at 10 K (solid line) and 300 K (dashed line). (b) 10-K middle-infrared absorption spectrum of $Na_2V_3O_7$ tube in a KCl pellet. The inset shows far-infrared transmittance ratios [$T(H)/T(H=0)$] at different applied magnetic fields at 4.2 K. The arrow indicates a 5% deviation from unity.

The middle-infrared absorption spectrum (Figure 4b) displays a total of 10 phonon modes.[53,54] Judging from a comparison with other model vanadates including V_2O_5, MV_3O_7 [M = CH_3NH_3or $N(CH_3)_4$], $(TMA)V_3O_7$, $(CH_3NH_3)_{0.75}V_2O_{10}\cdot 0.67H_2O$, and α'-NaV_2O_5,[29,55,56,58] the phonon modes of $Na_2V_3O_7$ can be sorted into three groups, with the centers of the three mode clusters located near 960, 850, and 620 cm^{-1}. Each group consists of three closely spaced but separate peaks. The triplet mode splitting in $Na_2V_3O_7$ is different from the response in other vanadates, and we attribute this splitting to the fact that three slightly different vanadium sites form the basic structural unit of the tube. We assign the highest-frequency triplet (999, 966, and 945 cm^{-1}) as stretching modes of the V−O (apical) bonds in the VO_5 square pyramids. Weak shoulders at 975 and 932 cm^{-1} might indicate the presence of slightly distorted pyramidal units. We assign the clusters at (883, 850, and 804 cm^{-1}) and (681, 619, and 571 cm^{-1}) as stretching modes of the edge- and corner-sharing V−O (basal) bonds, respectively. In addition to three sets of phonon modes, there is a small feature at 914 cm^{-1}. A similar peak has been observed on the low-frequency shoulder of the V−O (apical) stretching mode in other vanadate compounds,[29,56] although no assignment has been suggested.

As shown in Figure 4a, the far-infrared spectrum displays several phonon modes between 170 and 380 cm^{-1}, as well as a fairly isolated feature at 88 cm^{-1}.[59] We assign the structures between 170 and 380 cm^{-1} as V−O bending modes. The 88-cm^{-1} feature is interesting and merits extended discussion. We display a close-up view of this spectral range in the lower inset of Figure 4a. Unlike the other vibrational modes observed in $Na_2V_3O_7$, the oscillator strength of the 88-cm^{-1} peak exhibits a strong temperature dependence. The integrated intensity (upper inset, Figure 4a) saturates near 100 K. Interestingly, this saturation seems to correlate with a peak in the spin−lattice relaxation rate, observed in recent NMR measurements.[33]

Previous infrared studies of other vanadates indicate that the lowest-frequency modes are not due to localized vibrations of vanadium and oxygen atoms, as described previously, but instead are related to more complicated, long-range external motions such as translation, rotation, or liberation.[55,60] For instance, the 74-cm^{-1} feature in V_2O_5 is assigned as a rotational mode of $(V_2O_5)_n$

(53) The observed phonon modes are at 999, 966, 945, 914, 883, 850, 804, 681, 619, and 571 cm^{-1}. In addition, the 966-, 945-, and 850-cm^{-1} features have shoulder peaks.

(54) Our variable-temperature infrared work shows the usual mode narrowing with decreasing temperature; we find no evidence for any structural phase transitions in our investigated temperature range.

(55) Popova, M. N.; Sushkov, A. B.; Golubchik, S. A.; Mavrin, B. N.; Denisov, V. N.; Malkin, B. Z.; Iskhakova, A. I.; Isobe, M.; Ueda, Y. *J. Exp. Theor. Phys.* **1999**, *88*, 1186.

(56) Zhang, F.; Zavalij, P. Y.; Whittingham, M. S. *Mater. Res. Bull.* **1997**, *32*, 701.

(57) The number of heat-carrying phonons is linearly proportional to the temperature; thus the rattler's collision rate increases with increasing temperature.

(58) Chirayil, T.; Zavalij, P.; Whittingham, M. S. *Solid State Ionics* **1996**, *84*, 163.

(59) The strong background absorption appearing in the far-infrared spectrum is due to absorption and scattering by the paraffin matrix.

(60) Abello, L.; Husson, E.; Repelin, Y.; Lucazeau, G. *Spectrochim. Acta* **1983**, *39A*, 641.

chains.[60] Further, the 90-cm^{-1} mode in α′-NaV_2O_5 is attributed to translation of V_2O_5 units along the *c* axis; this motion can also considered as a translation of the (VO_5) chain, as the V_2O_5 units are connected along the *b*-axis ladder direction.[55] However, because of the title compound's tubular morphology, it is less likely that the 88-cm^{-1} mode can be attributed to the translation of V_2O_5 units. Thus, we considered in turn several low-energy excitations that might be connected with the unique tubular structure and magnetic character of $Na_2V_3O_7$, including translational motion of the tube, a radial or longitudinal breathing mode, rattling of Na^+ inside the tube, and a spin gap. We combined our results with previous measurements to identify a mechanism that supports our findings. Of these possible explanations for the behavior of the 88-cm^{-1} mode, the observed temperature dependence (insets, Figure 4b) makes the first two less likely, as tube translation and breathing motions are expected to display limited temperature effects.[61−65] Thus, we concentrate our discussion on the 88-cm^{-1} mode; analyze it as a rattling mode; and, at the same time, investigate the possibility of a spin gap assignment.

Rattling modes have been extensively studied on filled skutterudites (RM_4X_{12}, where R = rare-earth or actinide; M = Fe, Ru, or Os; X = P, As, or Sb) and clathrates ($X_8Ga_{16}Ge_{30}$) of interest as thermoelectric materials.[66,67,69−73] In these compounds, the guest atom (R in a filled skutterudite or X in a clathrate) undergoes large localized vibrations in an oversized atomic cage formed by other atoms, thus earning the name "rattler". From the mode dispersion point of view, the rattling mode is a mixture of both acoustic and optic modes, which, despite the radically different energy scale, undergo hybridization. The characteristic frequency can be estimated from the Einstein temperature, using $U = h^2T/(4\pi^2 m k_B \Theta_E^2)$, where *U* is the mean square displacement amplitude of a harmonic oscillator; *h* and k_B are the Planck and Boltzmann constants, respectively; *m* is the mass of the rattler; and Θ_E is the Einstein temperature.[74,75] With the known value of $U = 0.066$ $Å^2$ at 300 K for Na^+ atoms inside the $Na_2V_3O_7$ tubes,[26] the corresponding rattling frequency is 71 cm^{-1}. Here, we have assumed that there is no static disorder in the crystals. The reasonable agreement between the calculated rattling frequency and the observed 88-cm^{-1} peak supports the possibility that this feature is a Na^+ rattling mode. Note also that a rattling ion is only weakly bound; therefore, the "bond length" can be considered to be larger than the sum of the ionic radii (and likely more than the ∼5-Å cage diameter in these vanadate tubes). Judging from the shape of the thermal ellipsoid determined from X-ray measurements [U_{11} = 0.063(5) $Å^2$, U_{22} = 0.063(5) $Å^2$, U_{33} = 0.080(2) $Å^2$], Na^+ seems to move in all directions, with only slight preference to the direction along the tube. Unfortunately, the mode polarization cannot be confirmed from our far-infrared studies because of the isotropic nature of our pellet sample.

To our knowledge, the variable-temperature spectral response of rattling mode behavior in filled skutterudites or clathrates has not been investigated; such a comparison would obviously be extremely revealing. Nevertheless, the observed temperature dependence of the 88-cm^{-1} mode in $Na_2V_3O_7$ (insets, Figure 4a) contains a few clues that can support the aforementioned Na^+ rattling mechanism. For instance, the change in dynamics of the 88-cm^{-1} mode near 100 K (upper inset, Figure 4a) might signal a characteristic energy scale where the rattler moves away from the center of the ∼5-Å tube "pocket" and starts sampling potential minima inside the tube. Such a multiwell potential surface has been observed for the clathrates[76,77] and might be expected in the $Na_2V_3O_7$ system as well. If the rattler falls into an off-center potential well below 100 K, its fate (whether trapped or able to tunnel) will depend on the depth of the well. The lack of frequency shift, however, suggests that the rattler is not trapped. Low-temperature neutron scattering experiments should be able to shed light on the exact location of the Na^+ ion and the tunneling rate between such off-center sites. The observed temperature dependence of the 88-cm^{-1} mode might also be explained by a rattler's collision with heat-carrying phonons,[57] where strong rattler/phonon scattering could cause the reduction of the mode intensity at high temperatures. An alternate interpretation might follow that of recent NMR and dc-susceptibility measurements, correlating the quenching of the majority of V magnetic moment with a weak dimerization,[33] although our infrared measurements do not support this proposed dimerization. Measurements on larger-diameter alkali−vanadate tubes or exchange of the alkali metal for a different counterion should also allow us to distinguish between these different pictures.

Magnetooptics experiments provide additional support for the assignment of the 88-cm^{-1} feature as a Na^+ rattling mode in the tube. The inset of Figure 4b displays the transmittance ratio spectra of $Na_2V_3O_7$ nanotubes in several different applied magnetic fields

(61) The intensity of a librational mode (and a radial breathing mode in carbon nanotubes) is temperature-dependent as it increases with increasing temperature. Temperature change also leads to a frequency shift in carbon nanotubes.[62−65]

(62) Ross, S. D. *Inorganic Infrared and Raman Spectra*; McGraw-Hill: New York, 1972; Chapter 3.
(63) Sokhan, V. P.; Nicholson, D.; Quirke, N. *J. Chem. Phys.* **2000**, *113*, 2007.
(64) Huang, F.; Yue, K. T.; Tan, P.; Zhang, S.-L.; Shi, Z.; Zhou, X.; Gu, Z. *J. Appl. Phys.* **1998**, *84*, 4022.
(65) Huong, P.; Cavagnat, R.; Ajayan, P. M.; Stephan, O. *Phys. Rev. B* **1995**, *51*, 10048.
(66) The characteristic low frequency of the rattler enables it to scatter the heat-carrying phonons and therefore results in low lattice thermal conductivity.
(67) The physical properties of hexaborides are also dominated by rattling.[68]
(68) Mandrus, D.; Sales, B. C.; Jin, R. *Phys. Rev. B* **2001**, *64*, 12302.
(69) Sales, B. C.; Mandrus, D.; Williams, R. K. *Science* **1996**, *272*, 1325.
(70) Sales, B. C.; Mandrus, D.; Chakoumakos, B. C.; Keppens, V.; Thompson, J. R. *Phys. Rev. B* **1997**, *56*, 15081.
(71) Mahan, G. D.; Sales, B. C.; Sharp, J. *Phys. Today* **1997**, *Mar*, 42.
(72) Nolas, G. S.; Cohn, J. L.; Slack, G. A.; Schujman, S. B. *Appl. Phys. Lett.* **1998**, *73*, 178.
(73) Cohn, J. L.; Nolas, G. S.; Fessatidis, V.; Metcalf, T. H.; Slack, G. A. *Phys. Rev. Lett.* **1999**, *82*, 779.
(74) Sales, B. C.; Mandrus, D.; Chakoumakos, B. C. *Recent Trends in Thermoelectric Materials Research II*; Tritt, T. M., Ed.; Academic Press: New York, 2001; Vol. 70, Chapter 1, pp 1−34.
(75) The "rattling" motion is well described by an Einstein oscillator model. This equation is valid in the high-temperature limit, where $h\nu \ll 2mk_BT$.
(76) Chakoumakos, B. C.; Sales, B. C.; Mandrus, D. G. *J. Alloys Compd.* **2001**, *322*, 127.
(77) Sales, B. C.; Chakoumakos, B. C.; Jin, R.; Thompson, J. R.; Mandrus, D. *Phys. Rev. B* **2001**, *63*, 245113.

up to 17 T. If the 88-cm^{-1} feature is related to the predicted spin gap, the signature will change with field; Zeeman splitting of such structures has been observed in other low-dimensional magnetic materials in the past.[78] Judging from the lack of field-dependence in the transmittance ratio spectra near 88 cm^{-1}, we conclude that this feature is not related to the spin gap. Moreover, no evidence for a spin gap is observed within our sensitivity[79] over the investigated frequency range. This is in contrast to theoretical predictions of a spin gap, suggesting that the gap might be smeared as a result of small nonstoichiometric concentrations of Na^+, that it might lie in the millimeter frequency regime, or that $Na_2V_3O_7$ does not have a spin gap at all.

IV. Conclusion

We report the electrodynamic response of $Na_2V_3O_7$ over a wide frequency range in order to explore the electronic and vibrational structure of these new inorganic nanotubes. The electronic absorption spectrum shows a broad 1.2-eV band due to V d → d excitations and higher-energy bands at 3.3 and 3.9 eV that we assign as O p → V d charge-transfer transitions. Despite the additional predicted electronic confinement in $Na_2V_3O_7$ due to the tubular morphology, the similarities between the title compound and other layered and nonlayered vanadates are striking. Vibrational modes in the middle-infrared region, related to V−O stretching motion, display triplet splitting as a consequence of three distinctly different vanadium atoms that form the basic structural unit. The far-infrared response shows a number of V−O bending modes as well as a strongly temperature-dependent feature at 88 cm^{-1}, which we assign as a rattling mode of Na^+ in the tube. An estimate of the characteristic Einstein temperature, from which we extract a rattling frequency, is in line with this assignment.

Acknowledgment. This work was supported by the Materials Science Division, Office of Basic Energy Sciences, U.S. Department of Energy, under Grants DE-FG0201-ER45885 (University of Tennessee) and DE-FG05-86ER45259 (North Carolina State University). The National High Magnetic Field Laboratory in Tallahassee, Florida, is supported by the National Science Foundation and the State of Florida. We thank G.-H. Gweon, D. Mandrus, and B.C. Sales for useful discussions.

CM010965X

(78) Jones, B.; Sushkov, A. B.; Musfeldt, J. L.; Revcolevschi, A.; Dhalenne, G. *Phys. Rev. B* **2001**, *63*, 134414.

(79) The signal-to-noise ratio in our high-field experiments was less than 4%.